Mem. S.A.It. Vol. 74, 253

Memorie della

Star formation from ISO to HERSCHEL

P. Saraceno, L. Spinoglio and S. Molinari

Istituto di Fisica dello Spazio Interplanetario - CNR, via del Fosso del Cavaliere, 100, 00133 Roma, e-mail: saraceno@ifsi.rm.cnr.it

Abstract. ISO observations have shown that the far-infrared spectral range is the best window to observe pre-stellar and young stellar objects, because they emit the bulk of their energy in this region. The next far infrared and submillimeter mission of ESA Herschel will have a definitely better sensitivity and better spatial resolution compared to ISO. In this presentation we will discuss two observational key programs that can be performed with Herschel: the study of the nearby (d < 500pc) clusters and proto-clusters and the survey of the galactic plane.

Key words. infrared: general – stars: formation – infrared: stars – infrared: ISM – submillimeter – instrumentation: spectrographs – techniques: photometric

1. The two satellites

Figure 1 shows the pictures of ISO (Infrared Space Observatory), launched in 1995 and of Herschel, the following ESA mission, that will be launched in 2007. The two satellite are represented at the same scale showing that, while the telescope diameter increases of a factor ~ 6 (from 0.6m to 3.5m), the volume does not change of the same amount. ISO in fact had a cryogenically cooled (~ 4 K) mirror and most volume was taken by the helium tank, while Herschel will be radiatively cooled and the mirror size is close to the maximum possible with the available volume. For Herschel the amount of cryogen carried on board is reduced in favor of a larger collecting area and a longer duration of the mission (the liquid He will be used only to cool the instrumentation). The next step will be to use cryo-coolers on board. The Herschel mission will last a minimum of 3 years and its large mirror will increase the spatial resolution in the FIR and extend the spectral range to ~ 600 μm.

With a 4 K optics it was possible for ISO to reach the detectors noise limit, while Herschel, in the wide-band observations, will be limited by the photon noise of the $\sim$80 K optics. The collecting area of Herschel will compensate the higher temperature of the optics and, in the photometric bands in common with ISO (60 - 200 μm), it will be more sensitive by a factor larger than ten. Moreover from the difficulty found to understand the noise of the ISO detectors we learned that to reach the detector noise may not imply a great gain.

Three instruments are mounted on the focal plane of Herschel: two cameras (PACS and SPIRE) covering the 57-670 μm range, with broad-band and line imaging capabilities, spatial resolution close to the diffrac-

Send offprint requests to: P. Saraceno
Correspondence to: via del Fosso del Cavaliere, 100, 00133 Roma

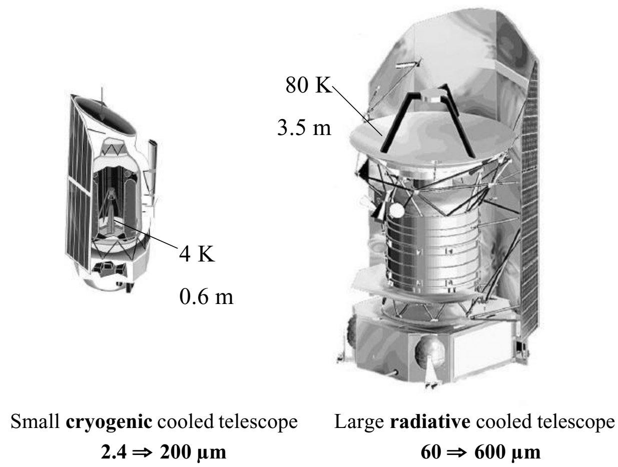

Fig. 1. Schematic view of ISO and Herschel

tion limit and a field of view of several arcminutes. The third instrument is an heterodyne spectrometer covering the 480 - 1910 GHz range (157 - 625 μm) with a spectral resolving power higher than 10^6.

In Tables I and II the sensitivities foreseen for SPIRE and PACS in broad-band photometric mode and in imaging spectroscopic mode are given. A detailed description of the Herschel instrumentation can be found in Griffin et al. (1998), Poglitsch (1998), de Graauw et al. (1998) and in the presentation of Tofani at this conference.

2. A comparison with ALMA

The uniqueness of the Far-Infrared (FIR) for star formation studies lies in its ability to discriminate among different evolutionary stages of young stellar objects (YSOs) and to define temperatures and masses of the circumstellar material and pre-stellar condensations (prior to the formation of the protostars). Fig. 2 shows that the spectral energy distributions (SEDs) of both protostars and pre-stellar condensations peak in the 100-200μm range, inside the ISO and Herschel bands. For comparison in Fig. 2 the bands of the sub-millimeter interferometer ALMA are also reported. ALMA will be available to the astronomical community nearly at the same time as Herschel, with higher sensitivity and spatial resolution, but with spectral bands situated in the Rayleigh-Jeans portion of the spectrum where different temperatures have similar colours, making difficult to measure the temperature, resulting in a high uncertainty in the mass estimate.

To further illustrate the potential of the FIR, in Fig. 3 we report the [60 - 100] versus [100 - 170] ISO-LWS colour-colour diagram (Pezzuto et al. 2002), for a sample of YSOs of different luminosity (from ~ 1 to 10^5 $L_\odot$) and different evolutionary stage (from 10^3 years to more than 10^7 years for T Tauri and Herbig AeBe stars). The different classes of objects occupy well separated areas of the plot, making this diagram a powerful probe to classify the objects and for deriving the evolutionary stage. If the same diagram would have been done using the ALMA colours, no separation among the different sources would be found.

Another advantage of Herschel with respect to ALMA is its larger field of view, making Herschel a definitely better instrument to survey large areas of sky.

In conclusion, ALMA will be the ultimate instrument to study in detail the morphologies of the pre-stellar condensations, but only the Herschel data will allow to

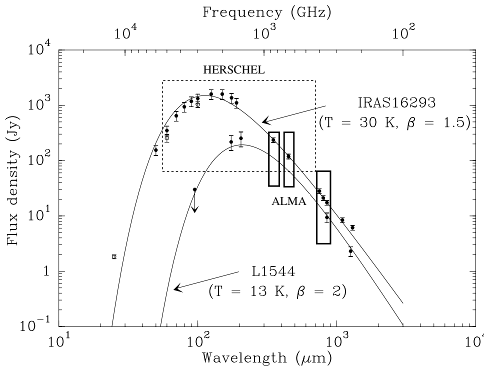

Fig. 2. Spectral energy distribution of the Class 0 protostar IRAS16293 and of the prestellar core L1554 obtained from ISO and JCMT observations, fitted with a simple gray body. The Herschel spectral band and the three high frequency bands of ALMA are reported on the figure (adapted from André et al. 2000).

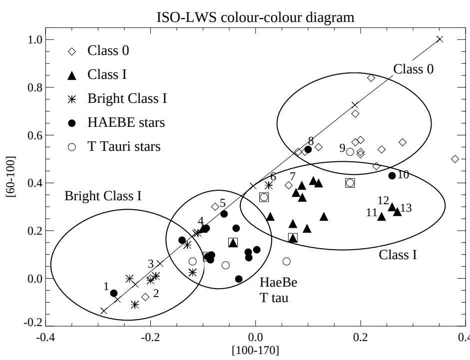

Fig. 3. Two colours diagram of a sample of YSOs of different masses and evolutionary stages, observed with the ISO-LWS spectrometers; the spectra were averaged over 1 μm around the wavelength of the three PACS band. The line shows the blackbody colours from 25 to 90 K (adapted from Pezzuto et al. 2002).

define dust temperatures and masses and only the Herschel instrumentation will produce maps of large areas of the sky. Starting from these considerations, in the following we outline two key projects of high priority in the Herschel observational program: i) the study of star formation in clusters with PACS and SPIRE, and ii) the survey of the Galactic plane at 250, 350, and 500 μm with SPIRE, followed by PACS and HIFI follow-up of selected areas.

3. Star formation in clusters

The observed large fraction of stars belonging to multiple systems and the observational evidence that most stars form in clusters (Nordh et al. 1996; Lada et al. 1991; Wilking & Lada 1985, for Chamaleon, L1630 and Taurus, respectively) both suggest that star formation has to be understood inside clusters and that the interaction among the different objects of the clusters has to be considered. The study of star formation in clusters may help to understand two major problems:

i) the origin of the Initial Mass Function (IMF). Millimeter surveys of protoclusters (Testi and Sargent 1998; Motte et al. 1998; Johnstone et al. 2001) suggest that the mechanism that fixes the final mass of a star has to be found in proto-clusters, the first stages of cluster formation. But these surveys are affected by the large uncertainties in the masses determination, as discussed in the previous paragraph.

ii) the formation of massive stars. It is well known that massive stars form in clusters, but only recently it becomes evident that the mass of the most massive object of a cluster is intimately related to the properties of the hosting clusters and increases with the stellar density (Zinnecker et al. 1993): in the low mass star forming regions the average distance between stars is 0.3 pc (Gomez et al. 1993, for Taurus) ; in the intermediate mass (Herbig AeBe) star forming regions this distance ranges from 0.2 pc, for the less massive objects, to 0.06 pc for the most massive ones (Testi et al. 1999); finally, in the high mass star forming regions this distance is less than 15.000 AU (Herbig & Terndrup 1986, for Trapezium), of the order of the sizes of the stellar envelopes, making collisions among protostars highly probable during the star formation process. Observations of young

Table I. Herschel, broad band imaging: foreseen sensitivity, field of view (FOV), spectral and spatial resolutions.

Instr.	Band Center [μm]	$\lambda/\Delta\lambda$	FOV [Arcmin]	Pixel Resolut. [Arsec]	Sensitivity (1σ, 1h)† Point Sources [mJy]	Map of 1 FOV [mJy]
SPIRE	500	~ 3	4 x 8	36	0.5	1.2
	350	~ 3	4 x 8	25	0.4	1
	250	~ 3	4 x 8	18	0.4	0.8
PACS	170	~ 3	3.5 x 1.75	12	0.6	
	100	~ 3	3.5 x 1.75	7	0.6	
	75	~ 3	3.5 x 1.75	5	0.6	

†:*For SPIRE the sensitivity for a point sources is different from the one needed to map all the FOV*

Table II. Herschel, imaging spectroscopy: foreseen sensitivity, field of view (FOV), spectral and spatial resolutions.

Instr.	Band [μm]	Spectr. Resolut. [Km/s]	FOV [Arcmin]	Pixel Resolut. [Arsec]	Sensitivity (1σ, 1h) Point Sources [W/m^2]	Map of 1 FOV [W/m^2]
SPIRE	670 - 300	300 $\div$ 3000	2.6 x 2.6	25	4.9 x 10^{-18}	1.2 x 10^{-17}
	300 - 200	300 $\div$ 3000	2.6 x 2.6	18	5.4 x 10^{-18}	1.3 x 10^{-17}
PACS	210 - 110	$\sim$200	0.8 x 0.8	9.4	5 x 10^{-19}	
	100 - 72	$\sim$200	0.8 x 0.8	9.4	8 x 10^{-19}	
	72 - 55	$\sim$200	0.8 x 0.8	9.4	1.56 x 10^{-18}	

SPIRE uses a Fourier Transfer Spectrometer with two channels working in parallel; each exposure produces a 200 - 670 μm spectrum for each spatially resolved element. PACS uses a grating spectrometer with imaging capabilities; the 110 - 210 μm channel works in parallel with one of the other two; at each exposure a 72 - 210μm spectrum or a 55 - 72μm and a 110 - 210μm spectrum is produced for each spatially resolved element.

clusters and proto-clusters will then be a top priority for Herschel, whose high sensitivity (Table 1 and Fig. 4) will allow to detect a 10 K dust condensation of the order of the Jupiter mass at the distance of Orion. The observations of young stars is easier, because they peak in the FIR (Fig. 2) and low mass stars are much more luminous in the protostellar phase than during the M-S phase (Stahler 1998; D'Antona & Mazzitelli 1994). Therefore given the high density of stars in clusters the factor that will limit Herschel observations will be confusion (Franceschini et al. 1991) rather than sensitivity, even at the highest spatial resolution ($\sim$ 5"). This problem is very serious because protostars evolve fast (see, e.g. Saraceno et al. 1996) and objects in different evolutionary stages are found in the same beam. An example of the influence of confusion is given in the following section.

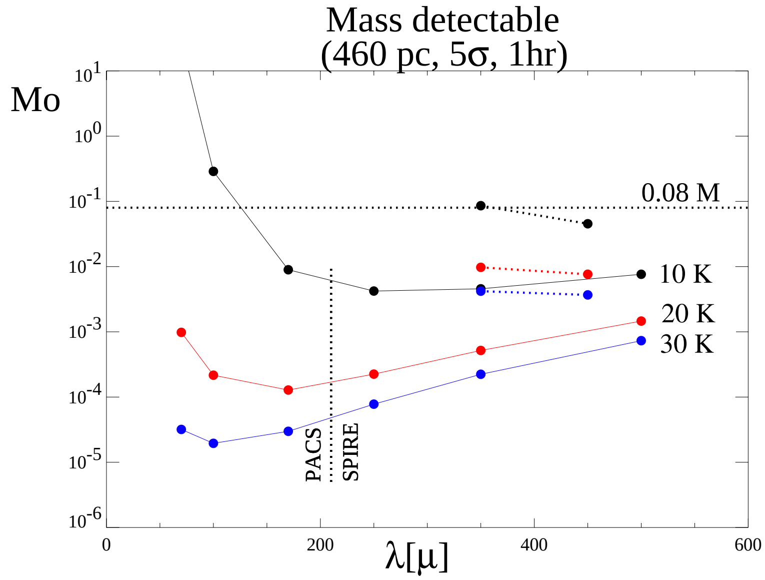

Fig. 4. Solid lines: the minimum detectable mass by Herschel computed for dust temperatures of 10, 20 and 30 K, as $M_{dust} = S_\nu \ D^2 \ /(k \ B_\nu)$ (Hildebrand 1983) where S_ν is the minimum detectable flux, D the distance of the cloud, k the dust emissivity and $B_\nu(T)$ the Planck function at the temperature T. The three dashed lines on the right give the limits of the SCUBA camera on the JCMT (15m) telescope. The horizontal dashed line correspond to the mass limit for Hydrogen ignition. At the distance of Orion all the spatially resolved proto-brown dwarfs should be detected by Herschel.

4. Simulated observation of a protocluster

In order to evaluate the confusion problems, we simulated an Herschel observations at 100 μm (with PACS), 250 and 500μm (with SPIRE) of the Serpens proto-cluster (d=350 pc). This region was mapped by Testi and Sargent (1998) with the OVRO interferometer at 3.4 mm with a resolution of 5.5" x 4.3" and a sensitivity of 3 mJy (similar to those of PACS). Fig. 5 (upper left panel) shows the published millimeter map with 26 condensations organized in two sub-clusters and (central upper panel) the derived mass function.

To simulate the sources that Herschel could detect, we extrapolate the derived mass function down to the mass that corresponds to a 50 mJy flux at 100μm, (assuming T_{dust}=20 K, k=0.005 cm^2/g, β=1.5), resulting in 220 extra sources (right upper panel). These sources, assumed point-like, were smeared with the diffraction pattern of the 3.5m telescope at the three wavelengths and added to the observed field with a 2D-Gaussian distribution around the 2 sub-clusters. Finally the noise expected for the needed integration times was added to the simulated fields. The results for the 100, 250 and 500μm bands are reported in the three lower panels of Fig. 5 and analyzed with DAOFIND to construct the mass function resulting from the simulated observations, that we compared with the input one (Fig. 6). The result shows that we missed ∼30 of the sources because of the limited spatial resolution, considerably affecting the determination of the mass function.

This very simple simulation shows that Herschel can detect many more sources than ground-based millimeter observations, producing large samples of high statistical

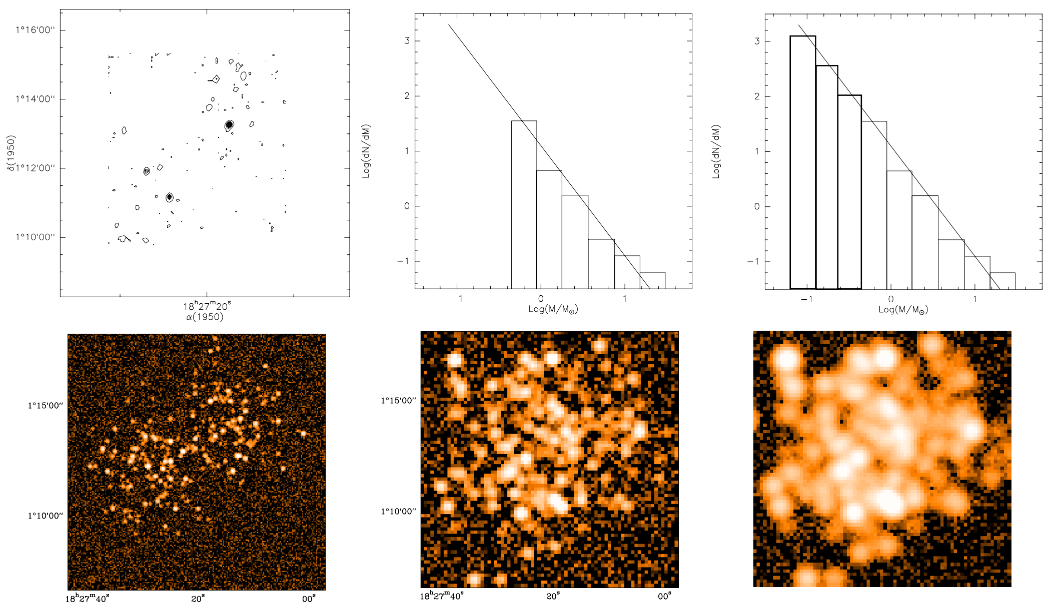

Fig. 5. Herschel simulated observations of the Serpens protocluster. Top-left : the 5'x 5' map of the Serpens cloud core observed at 3mm with the OVRO interferometer (Testi and Sargent 1998); resolution is 5.5" x 4.3" and limiting sensitivity is 3 mJy. Top-centre: the observed mass function. Top-right: extrapolated mass function. In the bottom panels the simulated fields at 100, 250, 500 μm are reported.

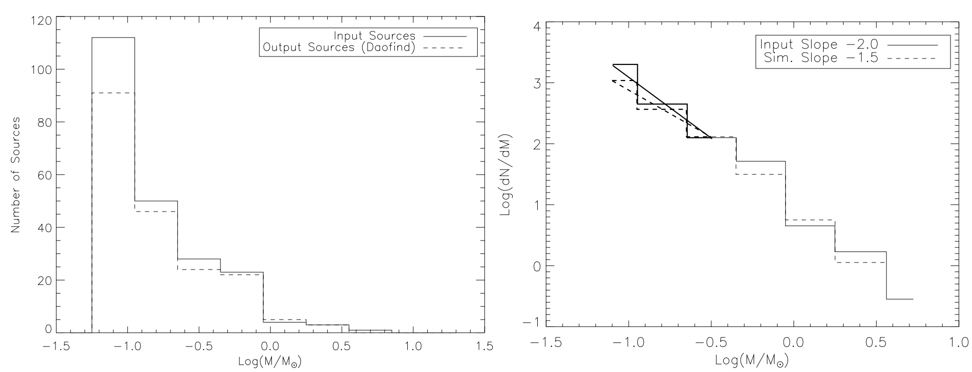

Fig. 6. On the left panel the input mass function, and the derived one (dot points) from the DAOFIND analysis, on the right, the effect on the derived mass function.

significance. The time needed to survey this area at a sensitivity of 50 mJy at 5σ is of $\sim$2 hours for the 60, 100, 170 μm bands (PACS) and of only 0.4 hours for the 250, 350, 500 μm of SPIRE. Since confusion will be the limiting factor, high priority should be given to all the nearby (d<500 pc) clusters and proto-clusters, where this problem is minimum.

5. Imaging spectroscopy

The ISO satellite has shown the great power of FIR lines to trace the warm gas of the star forming regions. The high spatial resolution of Herschel and its spectroscopic imaging capability will allow to trace the interactions among the members of a cluster. The spectroscopic imaging capability of Herschel will give for each spatially resolved element a full spectrum at intermediate spectral resolution tracing temperature, density and chemical composition. These informations are essential to study the ongoing physical processes (outflows, shocks, stellar winds, ionizing fields, etc.). Given the low extinction of the FIR lines, it will be possible to trace the inner parts of the clusters obscured in the near infrared.

Moreover different pre-MS objects have very different spectra. As an example, in Fig. 7, the LWS spectra of 3 objects are reported: a Class 0 (L1448mm, Nisini et al. 1999), a Class I (IC1396N, Saraceno et al. 1996) and a high luminosity Class I (W28A2, a very young star of $10^5 L_\odot$). The figure shows very different spectra, due to the different interactions of the objects with the ISM. The Class 0 and the low luminosity Class I have very rich spectra with several molecular transitions due to the presence of low velocity C shocks (Kaufman et al. 1996). On the contrary, the high luminosity Class I shows weak molecular lines, as expected by the presence of a strong UV field (Giannini et al. 1999). In these objects the atomic lines are the major coolants. All these conditions can be traced by the imaging spectroscopy of Herschel with a pixel resolution of ~9 arcsec (Table II).

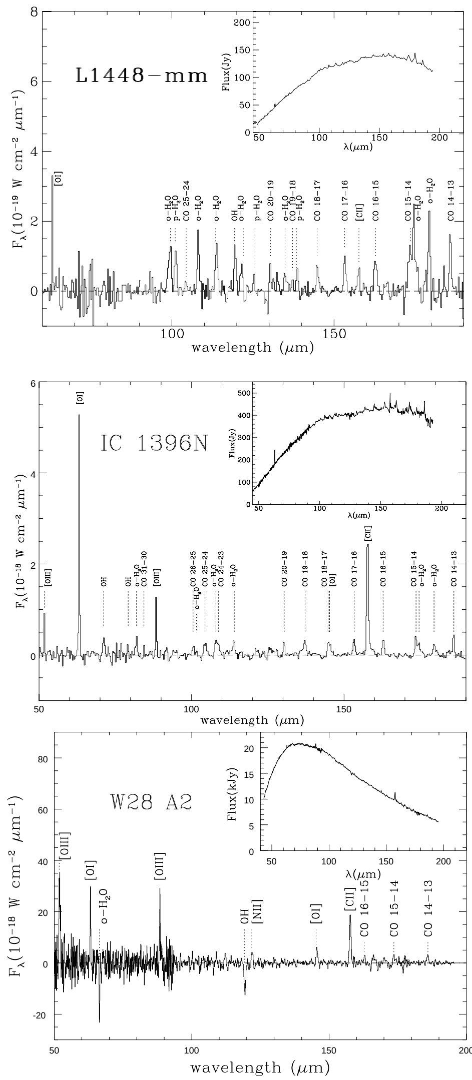

Fig. 7. FIR spectra of young stellar objects, from top to the bottom: objects: a Class 0 (L1448mm), a low luminosity Class I (IC 1396N) and a high luminosity Class I (W28 A2)

6. A Survey of the Galactic Plane

The complete survey of the galactic plane and the census of the Galactic star forming regions in a wide range of masses and evolutionary stages is one of the high priority programmes of Herschel. The mapping capabilities of the SPIRE instrument offer a unique compromise in terms of wavelength coverage (250, 350 and 500μm simultaneous mapping).

The thickness of the molecular component of the Galactic disk is ~70 pc (Blitz 1990), corresponding to ~2.5° at a distance

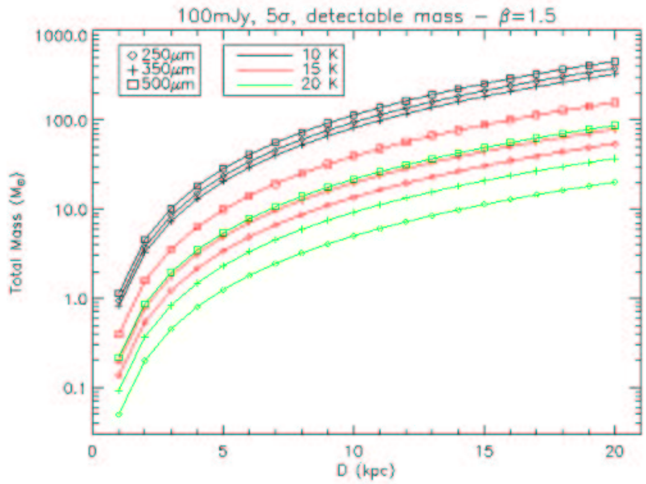

Fig. 8. Minimum (gas + dust) 5 σ detectable mass as a function of distance from the Sun, for the 3 photometric bands (indicated by the three symbols), and for three dust temperatures. A $\beta = 1.5$ is assumed for the dust emissivity-frequency law.

of 1 kpc. A 5°-wide band centered on the Galactic plane should then contain all star forming regions at a distance greater than 1 kpc. We can cover this region with a set of strips obtained by scanning the telescope along the b Galactic axis. Using the performances of Table 1, the full survey of the Galactic plane down to a sensitivity of 100 mJy, 5 σ in the 3 SPIRE bands can be completed in $\sim$ 70 days. This estimate assumes 21 hours/day observing time and includes 10 of overhead.

The potentiality of this survey is summarised in Fig. 6, where the flux sensitivity limit has been converted into total (gas+dust) detection limits at the 3 photometric bands for three different dust temperatures as a function of the distance from the Sun. Even a low-mass core like B335 (total mass of $3M_\odot$ and a dust temperature T $\sim$ 20 K) would be detectable at 250μm up to a distance of 10 kpc from the Sun.

PACS and HIFI follow-up investigations toward the most interesting areas are obviously foreseen.

Physical and evolutionary characterization of the detected sources will be optimized by cross-analyzing the survey database against similar databases in different wavebands but comparable spatial resolutions; obvious candidates for this type of study are the Midcourse Space Experiment (MSX, Shipman et al. 1996) 4.2-36μm survey of the Galactic plane, and the NRAO VLA Sky Survey (NVSS, Condon et al. 1998) at 6 cm for d=-40°.

References

André, P., et al. 2000, "Protostars & Planets IV", 59

Blitz, L. 1990, Star Forming Giant Molecular Clouds, in: Bloemen H. (ed.) The Interstellar Disk-Halo Connection in Galaxies, IAU Symp. 144, p.41

Condon, J.J., et al.. 1998, AJ 115, 1693

D'Antona, F., Mazzitelli, I. 1994, ApJ, 90, 467

de Graauw, T., et al. 1998, in Proc. SPIEE, 3357, 33

Franceschini, A., et al. 1991, A&AS, 89, 285

Giannini, T., et al., 1999, A&A, 346, 617

Gomez, M., et al. 1993, AJ, 105, 1927

Griffin, M.J., Vigroux, L., & Swinyard, B. M. 1998 Proc. SPIE, 3357, 404

Herbig, G.H., Terndrup, D.M. 1986. ApJ, 307, 609

Hildebrand, R.H. 1983. QJRAS, 24, 267
Johnstone D, et al. 2001 ApJ 559, 307
Kaufman, M.J., Neufeld, D.A. 1996, ApJ, 456, 250
Lada, E.A., Bally, J., and Stark, A.A. 1991, ApJ, 368, 432
Motte, F., André, P., and Neri R. 1998, A&A, 336, 150
Nisini, B., et al. 1999, A&A, 350, 529
Nordh, L., et al. 1996, A&A, 315, L185
Pezzuto, S., et al. 2002, MNRAS 330, 1034
Poglitsch, A. 1998, Proc. SPIE, 3354, 1032
Saraceno, P., et al. 1996, A&A, 315, L293
Shipman, Egan & Price 1996, BAAS, 28,1350
Stahler, W.S., 1988, ApJ, 332, 804
Testi, L., Sargent, A.I. 1998, ApJ, 508, L94
Testi, L., Palla, F., Natta, A. 1999, A&A, 342, 515
Wilking, B.A., Lada, C.J. 1985, "Protostars & Planets II",297
Zinnecker, H., et al. 1993, "Protostars & Planets III", 429